Jurnal Kejuruteraan 37(7) 2025: 3531-3541
https://doi.org/10.17576/jkukm-2025-37(7)-31

Partial Differential Solutions with Lumped Parameter Model for Single Phase Transformer Windings Voltage Distribution

Ramizi Mohame[da*], Syahirah Abd Halim[a], Khalil Azha Mohd Annuar[a] & Paul L. Lewin[b]

[a]*Department of Electrical, Electronic and Systems Engineering,*
Faculty of Engineering & Built Environment, Universiti Kebangsaan Malaysia, Malaysia

[b]*School of Electronics and Computer Science, University of Southampton,*
Southampton, SO17 1BJ, United Kingdom

[*]*Corresponding author: ramizi@ukm.edu.my*

Received 12 December 2024, Received in revised form 24 July 2025
Accepted 24 August 2025, Available online 30 October 2025

ABSTRACT

A high voltage transformer is one of the most critical components in power systems, responsible for regulating voltage levels and ensuring stable power delivery. Its main structure comprises the transformer core, voltage windings, insulation, metallic enclosure, and mechanical support. Over time, these components deteriorate due to thermal stress, mechanical strain, chemical aging, and especially voltage stress, which is a major contributor to insulation failure. Such failures can trigger partial discharges, inter winding faults, and eventual breakdown of the transformer windings. This paper presents a method for analyzing voltage distribution along transformer windings using partial differential equations (PDEs), providing greater insight into the effects of high-frequency transients. The methodology begins with a cross-sectional analysis of a single-phase transformer to extract physical and geometric parameters. An equivalent lumped parameter model comprising resistance (R), inductance (L), and capacitance (C) is developed to re lect the winding's electrical behaviour. The model is extended into a time-domain PDE framework, yielding two directional voltage wave solutions: one propagating toward the bushing, and the other toward the neutral terminal. Experimental validation was carried out by injecting a rectangular voltage wave and measuring the voltage response at several winding points. The results show strong correlation between theoretical predictions and experimental data, con irming the model's accuracy. The study highlights how voltage stress is unevenly distributed during fast transients, with certain winding sections experiencing elevated stress levels. This PDE-based approach enhances diagnostic accuracy and provides a valuable tool for assessing insulation performance, aiding in transformer design and predictive maintenance strategies.

Keywords: Partial differential solutions; lumped parameter model; transformer windings; Hybrid PDE

INTRODUCTION

Traditional transformer windings are constructed using large copper or aluminum conductors arranged in various configurations. These include helical, crossover, plain disc, and interleaved formations. Among these, plain disc and interleaved windings are the most widely used due to their ease of manufacture and straightforward representation as equivalent electrical circuits. The mechanical construction between the two looks very similar, but the only difference between the two is the interconnection at the edge windings that contributes to having more shunt equivalent capacitances for interleaved winding type (Mohamed 2010).

Apart from windings formation, second most important parameter is winding insulation. The role of transformer winding insulation is to insulate winding conductors and coils from short circuit with high property of breakdown voltage. Most of the transformer windings are made of cellulose-based material with high quality of insulation property as a dielectric material. This cellulose material is manufactured in the form of paper and is wrapped around the transformer windings. The solid conductor in transformer windings, along with the paper

insulation wrapped around it, can be represented as a lumped parameter circuit comprising a series of passive equivalent components like capacitances, inductances, and resistances. (Ramizi Mohamed et al. 2024; Ragavan & Satish 2007; Robak & Machowski 2024; Pramanik et al. 2022; Zhao et al. 2019).

The lumped parameter model has been widely used and invites some considerable interest in distribution transformer modelling. The study of lumped parameter model started with the investigation in two dimensional fields of transformer construction and design. The design lumped parameter model was associated to high frequency switching surges (Bewley, 1939). Not only restricted to high frequency oscillations, but the applications of lumped parameter model also has a major role in research investigation of transformer physical deformation mainly (Das & Fernandes 2023; Cheng et al. 2020; Wu et al. 2020).

Recent studies have underscored that frequency response analysis (FRA) alone cannot always capture the subtle, location dependent voltage gradients that develop during fast front stresses, especially in compact single-phase units now common in distribution networks. Pramanik et al. (2022) showed that even double ended FRA, while more sensitive to winding faults, still requires an a-priori calibration against a trusted electrical model to interpret the trace. Building on the analytical equations derived by Cheng et al. (2020), several authors therefore advocate hybrid approaches in which measured responses are "anchored" to a physically based lumped element network whose parameters follow the actual layer by layer geometry. Such links between experiment and model are vital, because they translate the purely spectral information of FRA into a spatial map of dielectric stress precisely the perspective needed when one wishes to predict where partial discharges (PD) will initiate during lightning impulses or converter driven over voltages.

Complementary work on grey box optimization and high frequency resonance prediction has further highlighted the limits of classical equivalent circuits. Aghmasheh et al. (2018), demonstrated that particle swarm optimisation can extract winding capacitances and inductances directly from design drawings, yet the resulting model still falters above a few hundred kilohertz where travelling wave effects dominate. Similarly, Davister et al. (2023) and Wu et al. (2020) showed that moisture ingress and cellulose ageing shift the natural frequencies enough to mask mechanical deformation in conventional diagnostics. The recent parameter interpolation method of Robak & Machowski (2024) partially alleviates this by refining leakage reactance estimates, but it remains a static technique. Taken together, these findings justify the present work use of a partial differential, travelling wave formulation anchored to a lumped network: it retains the geometrical intuition of the grey box models while extending their validity into the sub microsecond domain where insulation failure mechanisms truly begin.

The main contribution of this research lies in the development and implementation of a hybrid analytical numerical framework that enables detailed voltage distribution analysis along transformer windings under fast transient conditions. By integrating the classical lumped parameter model with the one-dimensional telegrapher's equation, the paper offers a novel yet computationally tractable method to predict localized overvoltages with improved spatial resolution. This approach bridges the gap between frequency-domain diagnostic methods and time-domain insulation stress analysis, thereby enabling a more accurate assessment of partial discharge risk and insulation ageing. Furthermore, the formulation facilitates practical validation using real transformer dimensions and electrical parameters, thus offering a pathway for integration into predictive maintenance and digital twin applications for high-voltage equipment.

Hence, this paper emphasizes a modeling technique for transformer windings based on their physical constructional design (Aghmasheh et al. 2018). The study compares the designs of single-phase transformers with interleaved and plain disc windings. To compare with, the methodology involved looking into the crossectional view between both windings. This technique highlights the differences in mechanical winding formation between plain disc and interleaved windings.

METHODOLOGY

SINGLE PHASE EXPERIMENTAL TRANSFORMER

The experimental transformer was based on a single phase model, designed by Tony Davies High Voltage Laboratory, University of Southampton (Han, B., 2004). The model includes both types of windings, as illustrated in Figure 1. The winding structure consist both interleaved and plain disc windings which interleaved windings was placed on top of plain windings. Both windings have similar construction size and use similar type of materials. In every winding, several terminals point of measurement is fastened connected internally and accessible to the outside container.

With reference to cross-sectional transformer windings of Figure 1, an equivalent arrangement of passive parameter capacitance, (C) and inductance, (L), can be drawn as shown in Figure 2. The parameter arrangement of L and C is based on transformer winding mechanical arrangement interconnected each other equals to its electrical parameters. The winding also shows and End Plate (EP) end connection

which is used to reduce the edge effects of transformer winding and also to reduce fundamental harmonic contents (Han, B. 2004).

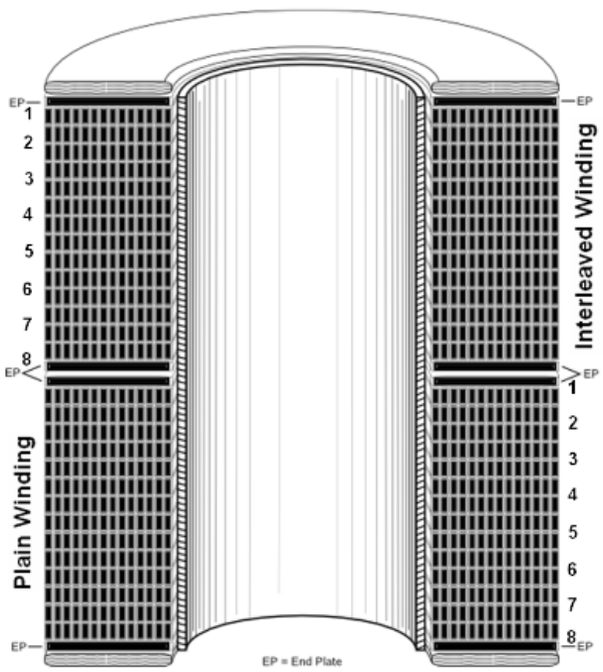

FIGURE 1. Crossectional view of interleaved winding and plain winding.

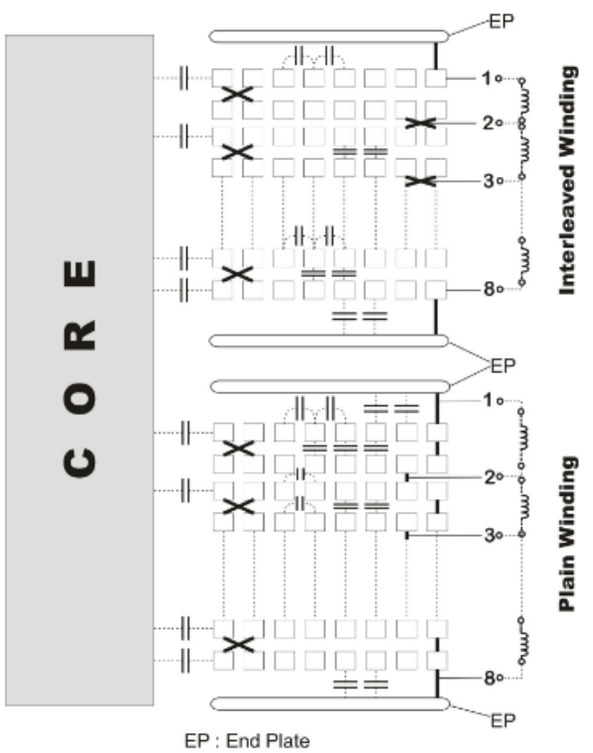

FIGURE 2. Equivalent *C, L*, parameter arrangement.

TRAVELLING WAVES IN TRANSFORMER WINDING

The voltage distribution along the transformer windings is often investigated using a non-invasive technique by injecting a rectangular wave. The used of rectangular wave is based on the specialty of its property with high transition time domain of voltage wavefront and an infinite wavetail. This will give good response in time domain, mimicking the physical parameter in its electrical equivalent.

SIGNAL INJECTION

Figure 3 shows a technique to inject a rectangular finite wave from typical function programmable function generator. As stated by Ramizi Mohamed et al. (2024), the finite rectangular wave algorithm can be generated by combining two exponential waves. When the wave is injected into the interleaved winding, the plain winding is short-circuited and grounded. Likewise, when the wave is injected into the plain winding, the interleaved winding is short-circuited and grounded. This approach is employed to eliminate the influence of mutual inductance between the two windings during measurements.

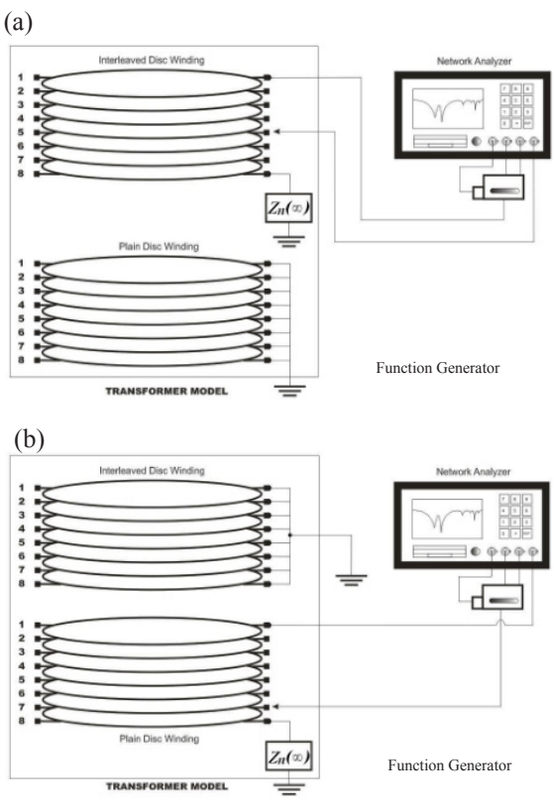

FIGURE 3. Arrangement of apparatus for signal injection a) signal injection for interleaved winding. b) signal injection for plain winding

TRANSFORMER MODEL WINDING WITH PARTIAL DIFFRENTIAL SOLUTIONS

Figure 2 shows internal crossection view for both plain disc windings and interleaved windings. From physical point of view the voltage level along the windings from point 1 to 8 may have similar distribution. If in any case the distribution may differ it is because of the end connection near the surface connections. This in turn may have different variation of inductance level due to interturn connection between disc connections.

To accurately model signal propagation within single-phase transformer windings, the physical windings are converted into an equivalent electrical circuit comprising passive components such as capacitances, inductances, and resistances. The equivalent circuit representation is illustrated in Figure 4. In this framework, both winding models share the same circuit structure, differing only in the values of their passive components.

As shown in Figure 4,
N - Neutral tap point,
B - Bushing tap point,
Cg - Capacitance between transmission and ground connection,
K – Capacitance between transmission segments.
x – Any distance along the single phase winding, where $x = 0$ at neutral tap point, and $x = l$ at bushing tap point.

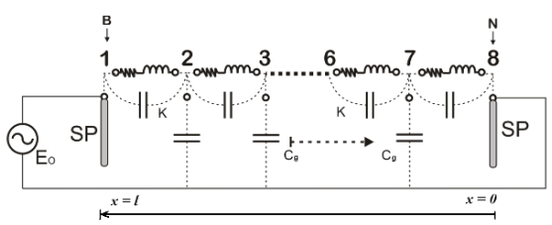

FIGURE 4. Representation of circuit for the three passive components (*RLC*).

TRANSMISSION OF AN INCIDENT WAVE AND SOLUTIONS TO THE PDE.

At time *t*, an arbitrary signal may be generated at any point *x*' along the transformer windings. This could result from faulty insulation system during live operation or from partial discharge occurrences under high voltage conditions. This will cause a divergence of current as shown in Figure 5. Equation 1 and 2 show the respective current divergence and PDE representation respectively.

With reference to Figure 5,
1. i_{kn} - Transmitted signal directed towards the neutral tap point.
2. i_{kb} - Transmitted signal directed towards the bushing tap point.

By considering the direction vector topology towards the neutral line to be positive, Equation (1) represents the divergence of the internal source current moving in both towards the bushing and towards the neutral end points. The divergence of current can be solved by using Kirchoff's Current Law (KCL) as followings:

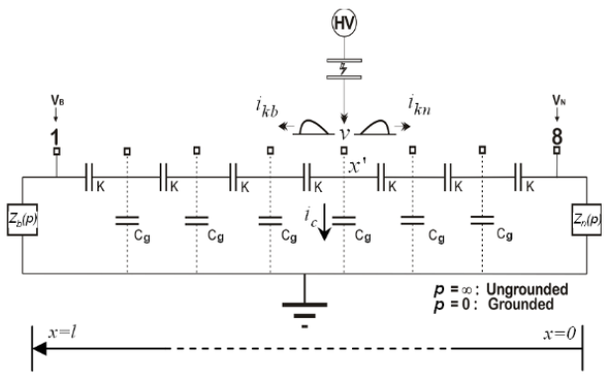

FIGURE 5. Signal divergence representation.

$$\nabla . i = 0 \tag{1}$$

Solving Equation (1) for all currents direction, the divergence of signal can be represented in PDE solution of Equation 2:

$$\frac{\partial i_k}{\partial x} + i_c = 0 \tag{2}$$

Where i_k is the current transmits through the capacitances between winding segments (K), and i_c is the current transmits through the shunt capacitances to ground (C_g). For which:

$$i_k = K \frac{\partial^2 v}{\partial x \partial t} \tag{3}$$

$$i_c = C_g \frac{\partial v}{\partial t} \tag{4}$$

Equations 2, 3, and 4 can be solved by eliminating the partial operator $\frac{\partial}{\partial t}$ from both sides of the equations. This results in a complete PDE solution as follows:

$$\frac{\partial^2 v}{\partial x^2} - \alpha^2 v = 0 \tag{5}$$

Where v is voltage level division along the transformer winding, α, is an arbitrary constant introduced known as fixed distribution constant:

$$\alpha = \sqrt{\frac{C_g}{K}} \quad (6)$$

Referring to Figure 5:

1. v_b: represents the voltage level along the single phase winding towards the bushing tap point.
2. v_n: represents the voltage level along the single phase winding towards the neutral tap point.

The terms v_b and v_n can correspo distance ranges along the transformer v

$$v_b; \quad x' \leq x \leq l \quad (7)$$

$$v_n; \quad 0 \leq x \leq x' \quad (8)$$

By solving the PDE equations in (5), the standing wave solution for the transformer windings will have a solution towards Neutral as:

$$v_n(x) = A\cosh(\alpha x) + B\sinh(\alpha x) \quad (9)$$

Tentatively, the standing wave solution towards Bushing can be represented as:

$$v_b(x) = \check{A}\cosh(\alpha x) - \check{B}\sinh(\alpha x) \quad (10)$$

Consider V_{sec} as the voltage distribution per section along the transformer windings. By applying Kirchhoff's Voltage Law (KVL), the derivation for the standing wave solution towards the bushing is as follows:

$$\alpha\check{A}\cosh(\alpha x) - \alpha\check{B}\sinh(\alpha x) + V_{sec} = 0 \quad (11)$$

Where A, $\check{A}$, B and $\check{B}$ are considered as arbitrary constants. Then by solving equations (10) and (11) simultaneously, the general standing wave solution in the direction towards bushing point can be represented as:

$$v_b(x) = C\,sech(\alpha x) - D\tanh(\alpha x) \quad (12)$$

Similarly, the constants of C and D are considered arbitrary that can be represented as:

$$\mathrm{C} = \check{A} \quad (13)$$

$$\mathrm{D} = \frac{V_{sec}}{\alpha} \quad (14)$$

With reference to the Equations (9) and (12), both are subject to conditional boundary values of the followings:

$$v_b(x) = V_B \ at \ x = l \quad (15)$$

$$v_n(x) = V_N \ at \ x = 0 \quad (16)$$

$$v_b(x) = v_n(x) \ at \ x = x' \quad (17)$$

$$x' \quad (18)$$

g terminals, $Z_b(p)$ and $Z_n(p)$ represent dances for both bushing tap point and neutral tap point, respectively. These terminal points are associated with boundary condition values, V_B and V_N, which can be determined through measurement. Consequently, using the boundary conditions specified in equations (15) to (18):

$$\mathrm{A} = V_N \quad (19)$$

$$C\,sech(\alpha l) - D\tanh(\alpha l) = V_B \quad (20)$$

And solving equation (18):

$$C\,sech(\alpha x') - D\tanh(\alpha x') = V_N\cosh(\alpha x') + B\sinh(\alpha x') \quad (21)$$

$$-C\tanh(\alpha x')\mathrm{sech}(\alpha x') - D\,sech^2(\alpha x') = V_N\sinh(\alpha x') + B\cosh(\alpha x') \quad (22)$$

Simultaneously solving equations (19) to (22) results in expressions:

$$B = C\,sech(\alpha x')\cosh(\alpha x') - D\,sech(\alpha x') - V_N\coth(\alpha x') \quad (23)$$

$$C = \frac{V_B\cosh(\alpha l)\sinh^3(\alpha x') - V_N\sinh(\alpha l)\cosh^2(\alpha x')}{\sinh^3(\alpha x') - [\cosh^2(\alpha x') + \sinh^2(\alpha x')]} \quad (24)$$

$$D = \frac{V_B\cosh(\alpha l)[\cosh^2(\alpha x') + \sinh^2(\alpha x')] - V_N\cosh^2(\alpha}{\sinh^3(\alpha x') - \sinh(\alpha l)[\cosh^2(\alpha x') + \sinh^2(\alpha x')]} \quad (25)$$

Where the variables B, C, and D are arbitrary constants. The solutions derived from equations (9) to (12) contain x'-dependent terms in each defined constant variable. This suggests that the winding distribution can be measured and determined based on the presented model

equations. These solutions effectively represent the voltage distribution from the bushing point (at the top of the transformer windings) to the neutral point (at the bottom of the transformer windings).

RESULTS AND DISCUSSION

The experiment depicted in Figure 3 aims to investigate the voltage level distribution along transformer windings for both interleaved and plain disc types. Understanding this voltage distribution is crucial for estimating potential current discharges within the windings. The transformer windings were tested using three different sampling times: 50 μs, 200 μs, and 350 μs, with the amplitudes analyzed in the time domain.

The experiment involves injecting a 5V measurable infinite rectangular signal with a 50 *ns* rise time at various terminals (1 to 8) along the transformer windings. Response measurements were recorded, and the amplitudes were noted for each signal injection. Throughout the process, the signal transition and the amplitude of the injected signal were maintained as consistently as possible to ensure uniform excitation across all measured winding terminals.

The result of the extracted amplitude for pattern model simulation is shown in Figure 6, based on the PDE model solutions derived in Equations 1 to 25. The fixed distribution constant is set to a value of $\alpha = 1.5$ based on its optimum level defined by Ramizi Mohamed et al. 2024 and Mohamed, R. 2010.

Based on the experimental observations, as the signal injection source moved from the terminal bushing to the neutral-grounded terminal points, the voltage distributions levelled out at the top of the winding where the injection was close to $x' = 7/7$. As the injection moved towards $x' = 0/7$, the voltage levels were damped to a very low level and approached zero level.

In comparison between figure 6 and figure 8, both the simulation and measurement results are in agreement. The PDE simulation model and the experimental results exhibit a similar pattern in voltage levels along the single phase transformer windings. The results taken for interleaved windings and plain disc windings were extracted for 0*s* to 450μs and at 0s to 45μs sampling time respectively with 10MS/s sampling rate. Meanwhile, the results shown in figures 6(h), 7(h) and 8(h) are correspond to measurements taken near the ground connection for the both simulation and experimental measurements, with a sampling time ranging between −9.4μs to 9.5μ*s*.

The proposed hybrid PDE framework with lumped parameter model stands out because it combines the physical intuition of classical ladder circuits with the wave propagation fidelity of the wave equation (Table 1). Unlike purely spectral methods (e.g., FRA) or static grey-box circuits, it can map voltage overshoots anywhere along the winding during nanosecond scale events which are precisely the conditions that initiate partial discharges and insulation ageing. While it still relies on accurate RLC data, its closed-form standing wave solution keeps computational effort low, making it suitable for digital-twin or on-line diagnostic platforms where speed matters.

The comparative table highlights the clear advantage of the proposed hybrid PDE-lumped parameter model in resolving high-frequency voltage dynamics along transformer windings. Traditional lumped parameter models, though widely adopted, only provide voltage values at discrete nodes and are limited in accuracy when dealing with transient phenomena beyond the first resonance. In contrast, the PDE-based approach introduced in this study offers continuous spatial resolution, enabling precise mapping of voltage peaks and gradients at any point along the winding. This is particularly relevant under fast front excitations where insulation stress is highly localized. Figures 6 and 7 illustrate this strength vividly, the voltage distribution curves reveal sharp transitions and standing wave patterns that would not be captured by conventional circuit models. The ability to resolve such fine-scale voltage variations is crucial for assessing partial discharge (PD) risk, as PD typically initiates at localized overstress points.

Moreover, the experimental validation shown in Figure 8 demonstrates excellent agreement between measured amplitude responses and the theoretical solution derived from the PDE formulation. The model accurately predicts both the timing and magnitude of voltage peaks along the winding under rectangular wave excitation, which mimics conditions experienced during lightning impulses or switching surges. Such fidelity is not observed in static grey-box or frequency-domain models, which either oversimplify the spatial aspect or ignore time-domain effects. By comparing the experimental results with the model predictions, the hybrid PDE approach proves to be a robust and practical diagnostic tool, bridging the gap between analytical clarity and physical realism. This supports the argument that for modern transformers subjected to fast transient conditions, spatially resolved time-domain modelling is essential for predictive maintenance and insulation reliability assessment.

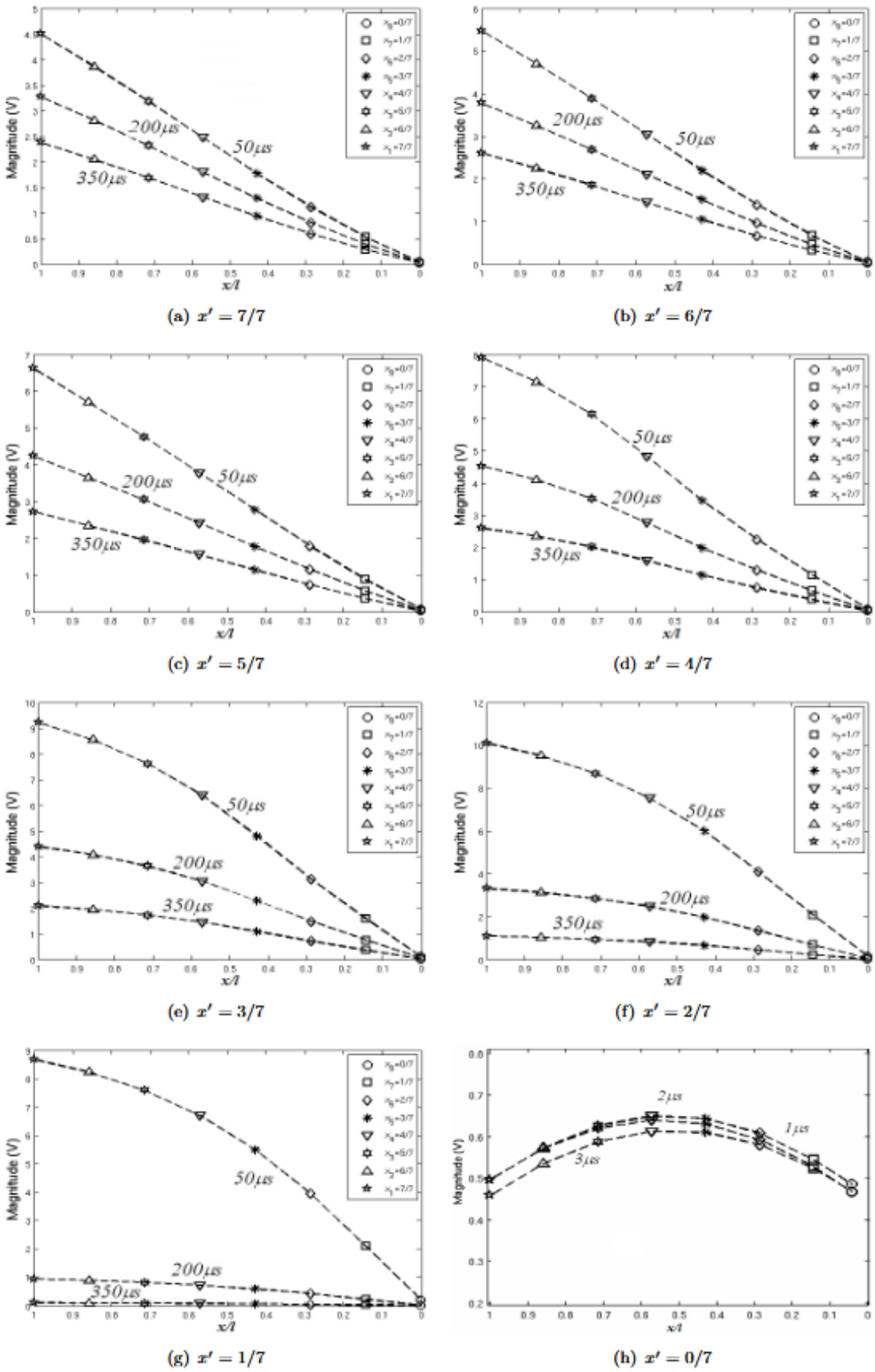

(a) $x' = 7/7$ (b) $x' = 6/7$

(c) $x' = 5/7$ (d) $x' = 4/7$

(e) $x' = 3/7$ (f) $x' = 2/7$

(g) $x' = 1/7$ (h) $x' = 0/7$

FIGURE 6. Voltage distribution representation based on PDE equation derivation.

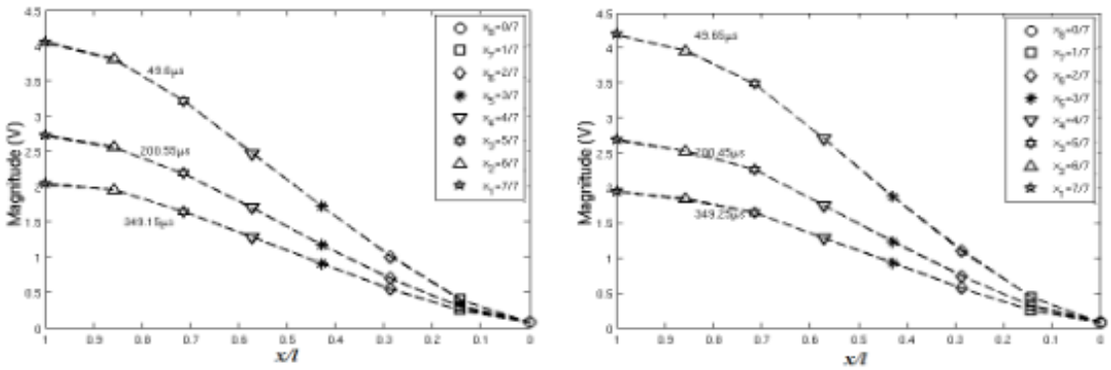

(a) $x' = 7/7$ (b) $x' = 6/7$

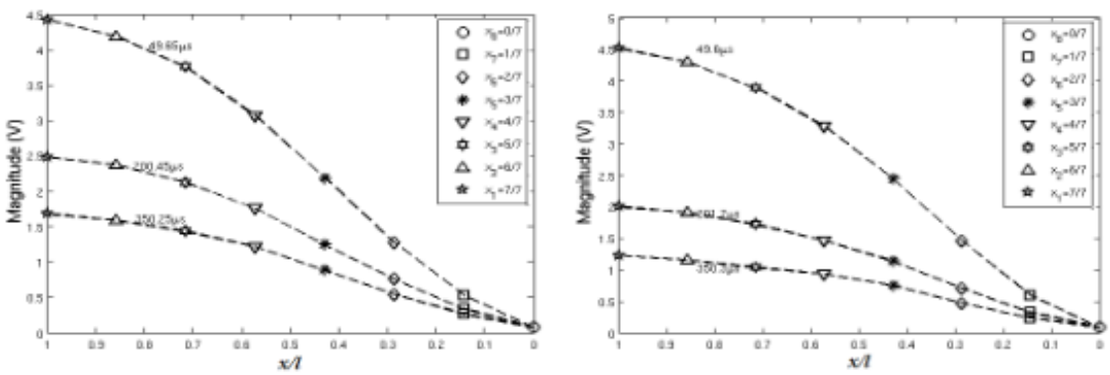

(c) $x' = 5/7$ (d) $x' = 4/7$

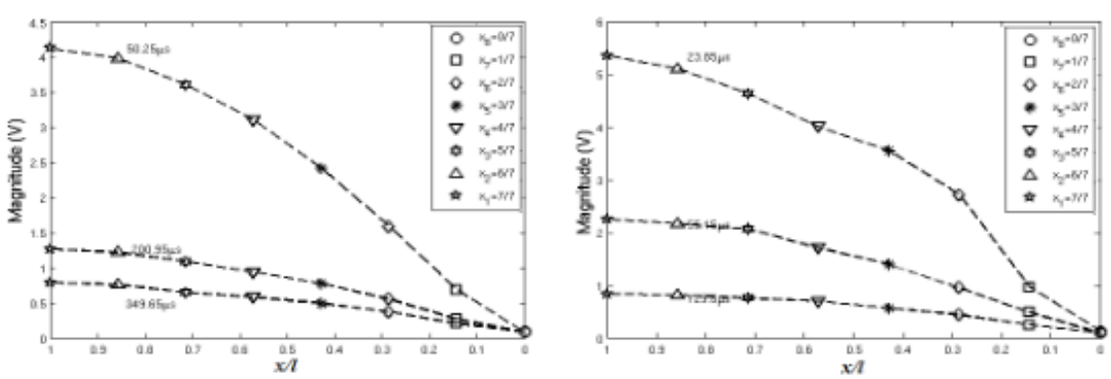

(e) $x' = 3/7$ (f) $x' = 2/7$

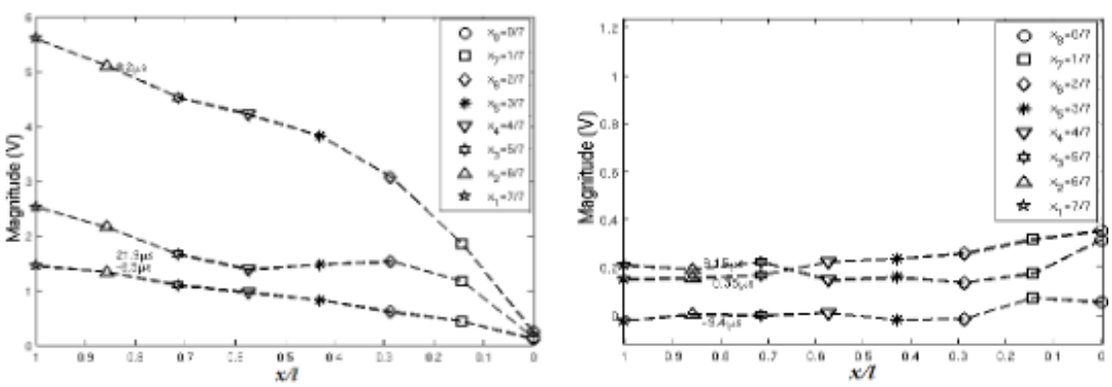

(g) $x' = 1/7$ (h) $x' = 0/7$

FIGURE 7. Voltage distribution representation of interleaved winding from measurement.

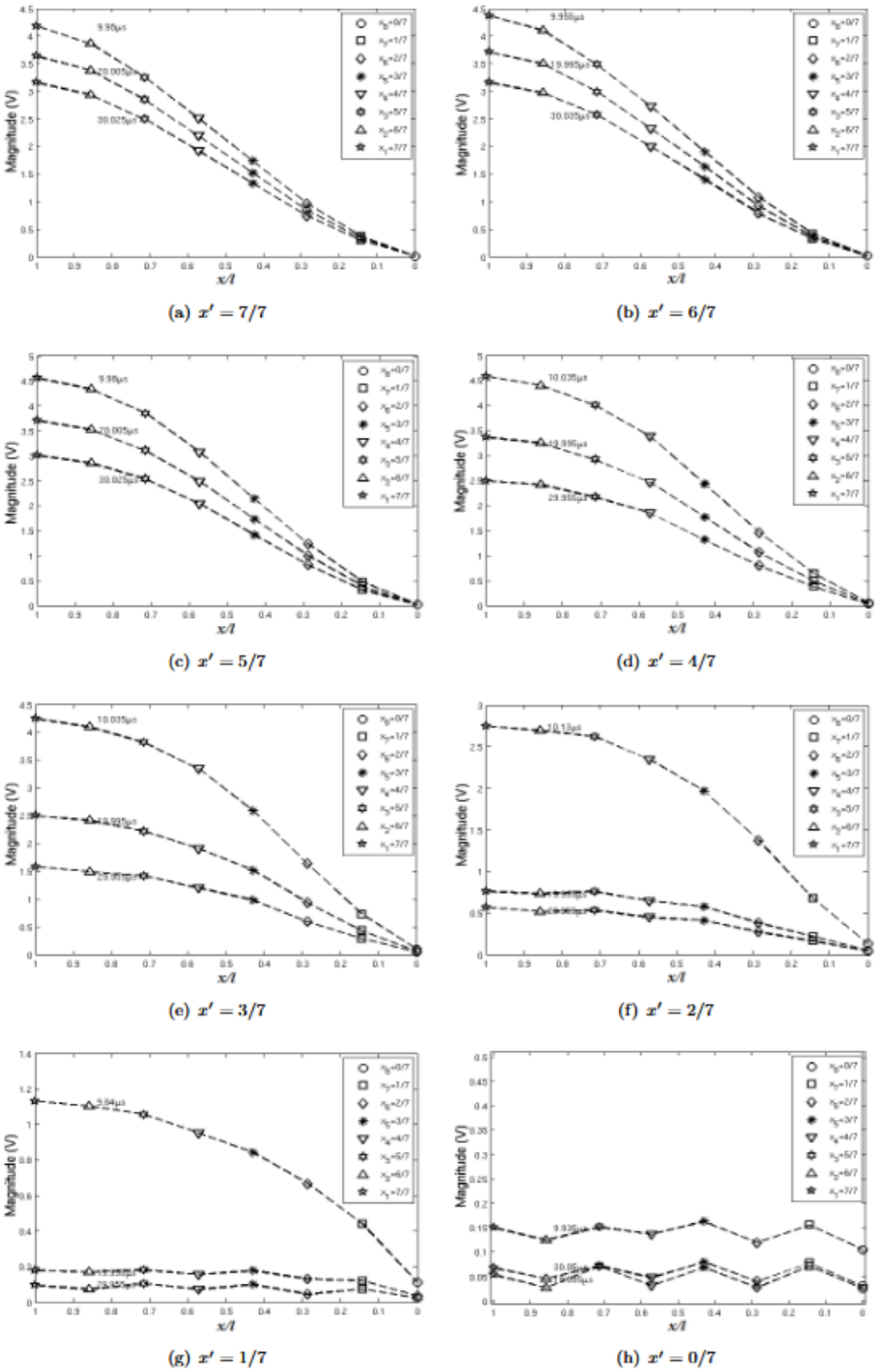

(a) $x' = 7/7$ (b) $x' = 6/7$

(c) $x' = 5/7$ (d) $x' = 4/7$

(e) $x' = 3/7$ (f) $x' = 2/7$

(g) $x' = 1/7$ (h) $x' = 0/7$

FIGURE 8. Voltage distribution representation of plain winding from measurement.

TABLE 1. Comparative overview of winding voltage models

Model / key reference	Core principle & domain of validity	Spatial detail along winding	Data & computation needed	Main strengths	Main limitations
Hybrid PDE – Lumped Parameter Model (this paper)	Couples a per-section RLC ladder to the one-dimensional waves equation; solutions give forward (bushing) and reverse (neutral) travelling-wave voltages	High: continuous profile resolved to any position *x*	Physical dimensions → R, L, C per section + two terminal impedances; closed-form standing-wave solution → low run-time cost	Captures sub-μs transients and non-uniform stresses; experimentally validated with rectangular-wave injection	Assumes insulation parameters remain constant (no real-time moisture/ mechanical change)
Classical lumped-parameter ladder (Bewley 1939; Cheng *et al.* 2020)	Pure RLC network solved in frequency domain; valid below first resonance (< 0.3–0.5 MHz for distribution units)	Low: voltage only at discrete nodes	Name-plate geometry or FRA curve ↔ parameter fitting; negligible computation	Simple, intuitive, widely used in design software	Neglects travelling-wave effects; accuracy degrades for fast transients
Grey-box PSO model (Aghmasheh *et al.* 2018)	Particle-swarm optimisation extracts R, L, C from drawings; still a static circuit	Low–medium (node voltages)	CAD drawings + measured terminal admittance; moderate optimisation cost	Automatic parameter tuning; good for design variants	Breaks down beyond a few hundred kHz; cannot predict wavefront steepening
Double-ended FRA diagnostic (Pramanik *et al.* 2022)	Measures magnitude/ phase response from both ends to detect deformation	None intrinsically (spectral only)	Network analyser sweep; minimal processing	Very sensitive to mechanical shifts; field-deployable	Needs a calibrated model to convert spectra to spatial faults; time-domain stresses not addressed
Parameter-interpolation refinement (Robak & Machowski 2024)	Uses Lagrange interpolation to adjust leakage reactance in three-winding ladders	Low (node voltages)	Name-plate data + power-frequency tests; analytic update	Improves accuracy at fundamental & harmonics without costly optimisation	Static, frequency-domain; offers no insight into fast front behaviour

CONCLUSION

A novel technique has been introduced to measure voltage distribution along transformer windings. This method is based on modeling the partial differential solution of a lumped parameter model, in hybrid way, primarily comprising capacitive passive elements that represent the paper insulation of windings in a single-phase power transformer. To validate the derived model, measurable rectangular waves were injected into two different types of winding models: interleaved winding and plain disc winding. The rectangular wave used has a unique characteristic of near-zero rise time, producing a distinctive excitation response in the wave tails. By utilizing sufficient information, including the values of shunt capacitance to ground (C_g) and series capacitance (K), the voltage distribution can be accurately estimated, assuming there is no mechanical movement or deformation that could alter the original insulation capacitance values.

ACKNOWLEDGEMENT

The authors would like to thank Universiti Kebangsaan Malaysia for the financial support and University of Southampton for the Laboratory facility.

DECLARATION OF COMPETING INTEREST

None.

REFERENCES

Aghmasheh, R. Rashtchi, V. & Rahimpour, E. 2018. Gray box modeling of power transformer windings based on design geometry and particle swarm optimization algorithm. *IEEE Transactions on Power Delivery* 33(5):2384-2393.

Bewley, L. V., 1939. Equivalent circuits of transformer and reactors to switching surges. *Transaction of Americal Institute of Electrical Engineering* 5:797-802.

Cheng, B. Wang, Z. & Crossley, P. 2020. Using lumped element equivalent network model to derive analytical equations for interpretation of transformer frequency responses. *IEEE Access*. 8:179486-179496.

Das, A. K. & Fernandes, B. G. 2023. An analytical method to obtain a wide frequency range equivalent π-Model of a two-winding medium/high-frequency transformer. *IEEE Transactions on Industry Applications* 59(6):7061-7077.

Davister, N. Henrotte, F. Frebel, F. & Geuzaine, C. 2023. Multiple resonance prediction through lumped-parameter modeling of transformers in high-frequency applications. *IEEE Transactions on Magnetics* 59(6):1-4.

Han, B. 2004. Partial Discharge Monitoring of Power Transformer. Doctor of philosophy, School of Electrical and Computer Science, University of Southampton, School of Electrical and Computer Science, SO17 1BJ, United Kingdom.

Mohamed, R. 2010. Partial Discharge Signal Propagation, Modelling and Estimation in High Voltage Transformer Windings, Doctor of Philosophy, School of Electrical and Computer Science, University of Southampton, SO17 1BJ.

Pramanik, S. Ganesh, A. & Duvvury, V. S. B. C. 2022. Double-end excitation of a single isolated transformer winding: An improved frequency response analysis for fault detection. *IEEE Transactions on Power Delivery* 37(1):619-626.

Ragavan, K. & Satish, L. 2007. Localization of changes in a model winding based on terminal measurements: experimental study. *IEEE Transactions on Power Delivery* 22(3):1557-1565.

Ramizi Mohamed, Syahirah Abd Halim & Paul L. Lewin. 2024. Winding response under difference effective inductance for single phase high voltage transformer. *Jurnal Kejuruteraan* 36(2):447-453.

Robak, S. & Machowski, J. 2024. Estimation of off-nominal parameters of three-winding transformers using Lagrange interpolation. *IEEE Transactions on Power Delivery* 39(3):1931-1938

Wu, Q. Hu, Y. Dong, M. Song, B. Xia, C. Yu, B. Zhang, Z., & Liu, Y. 2020. Optimization of Transformer Winding Deformation Assessment Criterion Considering Insulation Aging and Moisture Content. *Energies* 13(24):6491.

Zhao, J. Zirka, S. E. Moroz, Y. I. Arturi, C. M. Walling, R. A. Tleis, N. & Tarchutkin, O. L. 2019. Topological transient models of three-phase, three-legged transformer. *IEEE Access* 7:102519-102529.